

# Journal Pre-proof

Assessing the photocatalytic activity of europium doped TiO<sub>2</sub> using liquid phase plasma process on acetylsalicylic acid

Sang-Chul Jung (Conceptualization) (Investigation) (Data curation) (Writing - original draft) <ce:contributor-role>Writing - review and editing), Hye-Jin Bang (Investigation) (Data curation), Heon Lee (Investigation) (Data curation), Hyung-Ho Ha (Data curation) (Validation), Young Hyun Yu (Data curation) (Validation), Sun-Jae Kim (Data curation) (Validation), Young-Kwon Park (Conceptualization) (Data curation) (Validation) (Writing - original draft) <ce:contributor-role>Writing - review and editing)



PII: S0920-5861(20)30389-8

DOI: <https://doi.org/10.1016/j.cattod.2020.06.004>

Reference: CATTOD 12922

To appear in: *Catalysis Today*

Received Date: 28 February 2020

Revised Date: 9 May 2020

Accepted Date: 3 June 2020

Please cite this article as: Jung S-Chul, Bang H-Jin, Lee H, Ha H-Ho, Yu YH, Kim S-Jae, Park Y-Kwon, Assessing the photocatalytic activity of europium doped TiO<sub>2</sub> using liquid phase plasma process on acetylsalicylic acid, *Catalysis Today* (2020), doi: <https://doi.org/10.1016/j.cattod.2020.06.004>

This is a PDF file of an article that has undergone enhancements after acceptance, such as the addition of a cover page and metadata, and formatting for readability, but it is not yet the definitive version of record. This version will undergo additional copyediting, typesetting and review before it is published in its final form, but we are providing this version to give early visibility of the article. Please note that, during the production process, errors may be discovered which could affect the content, and all legal disclaimers that apply to the journal pertain.

© 2020 Published by Elsevier.

# Assessing the photocatalytic activity of europium doped TiO<sub>2</sub> using liquid phase plasma process on acetylsalicylic acid

Sang-Chul Jung<sup>a</sup>, Hye-Jin Bang<sup>a</sup>, Heon Lee<sup>a</sup>, Hyung-Ho Ha<sup>b</sup>, Young Hyun Yu<sup>b</sup>,

Sun-Jae Kim<sup>c</sup>, Young-Kwon Park<sup>d,\*</sup>

<sup>a</sup> Department of Environmental Engineering, Sunchon National University, 255 Jungang-ro, Sunchon, Jeonnam 57922, Republic of Korea

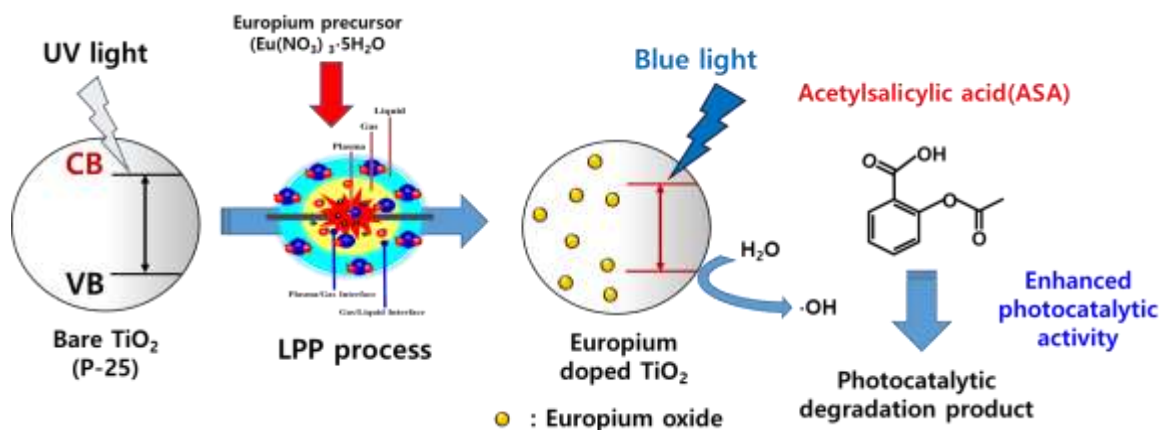
<sup>b</sup> College of Pharmacy, Sunchon National University, 255 Jungang-ro, Sunchon, Jeonnam 57922, Republic of Korea

<sup>c</sup> Faculty of Nanotechnology and Advanced Materials Engineering, Sejong University, 209 Neungdong-ro, Gwangjin-gu, Seoul 05006, Republic of Korea

<sup>d</sup> School of Environmental Engineering, University of Seoul, 163 Seoulsiripdaero, Dongdaemun-gu, Seoul 02504, Republic of Korea

\*Corresponding author e-mail: catalica@uos.ac.kr

## Graphical abstract



## Highlights

- LPP method synthesizes high efficiency visible light-responsive photocatalyst.
- The element Eu was distributed evenly on the  $\text{TiO}_2$  surface in oxide form.
- The higher the doping amount of Eu, the lower the band gap energy.
- The higher the doping amount of Eu, the better the photolysis activity.
- Two preferred routes were recommended for the photocatalytic degradation pathway.

## Abstract

In this study, europium (Eu) was precipitated in  $\text{TiO}_2$  powder using liquid phase plasma (LPP) process to prepare a photocatalyst with higher activity, even in the visible light range.

Eu was uniformly deposited on the surface of TiO<sub>2</sub> by the LPP method. It was observed that the amount of Eu precipitated on the TiO<sub>2</sub> surface increased with increasing precursor concentration. XPS and EDS analysis showed that Eu was precipitated as europium oxide. The precipitation of Eu shifted the position of the Raman peak to a higher wavelength; with higher Eu content, the band gap energy decreased. Particularly, the photocatalytic efficiency of the Eu doped TiO<sub>2</sub> photocatalyst (EDTP) in the visible light source was much higher than that of bare TiO<sub>2</sub>, and with higher Eu content, the photocatalytic activity was improved. Acetylsalicylic acid was attacked by HO· produced on the EDTP's surface and assumed to be finally mineralized to H<sub>2</sub>O and CO<sub>2</sub> *via* two decomposition pathways, namely, decarboxylation and deacetylation.

**Keywords:** TiO<sub>2</sub> photocatalyst, Liquid phase plasma, Acetylsalicylic acid, reaction rate constant, degradation mechanism

## 1. Introduction

Anti-inflammatory drugs (AIDs) are one of the most widely used drug groups in the world and have persistent toxicity [1]. About 50 kinds of AIDs are commonly used, such as aspirin, ibuprofen, and diclofenac. Aspirin, also known as acetylsalicylic acid (ASA), is derived from salicylic acid. Several studies have reported the presence of these pharmaceutical compounds in lakes, rivers, and freshwater environments [2–4].

Pharmaceutical wastewaters (PWWs) that contains recyclable and toxic organic compounds can lead to very serious water environmental problems [5]. These organics have a high

resistance to microbial degradation or utilization, especially at high concentrations [6]. Thus, increased emissions of PWW cannot be fully treated with conventional biological treatment alone [7]. To meet increasingly stringent discharge wastewater standards, these PWWs must be treated with powerful and advanced treatment technologies.

Recently, advanced oxidation processes (AOPs) have been applied to treat PWWs [8,9]. These processes use a variety of reactive radical species (e.g., hydroxyl and oxygen radicals) to effectively remove non-biodegradable contaminants from the water environment. Ozonation, Fenton reaction, ultraviolet (UV) decomposition, liquid phase plasma decomposition, and photocatalytic reactions are known as representative members of AOPs [10–13]. Among these processes, a combination of  $\text{TiO}_2$  as a photocatalyst and UV light has been found to degrade organic pollutants into biodegradable or inorganic materials ( $\text{CO}_2$  and  $\text{H}_2\text{O}$ ) using highly reactive hydroxyl radicals [14–16].

The most significant hurdle to the use of  $\text{TiO}_2$  as a photocatalyst is its large band gap (anatase: 3.2 eV, rutile: 3.0 eV) [17,18]. Owing to this large band gap,  $\text{TiO}_2$  photocatalysts should only utilize less than 5% of the UV radiation reaching the Earth's surface [19,20]. Thus, to overcome the limitations of the  $\text{TiO}_2$  photocatalyst, a system for adding hydrogen peroxide, ozone, and microwaves was introduced [21,22]. A fundamental solution is the doping of  $\text{TiO}_2$  with nonmetals, transition metals, and rare earth elements [23–25]. Of these, rare earth-doped  $\text{TiO}_2$  is known to have adsorption wavelength shifted to visible light region or to reduce electron-hole recombination. [26].

Among various doping techniques that are applied to  $\text{TiO}_2$  photocatalysts, a method of attachment using a plasma generated in a liquid phase has recently been attempted [27–29]. Liquid phase plasma (LPP) methods have been applied to prepare nanocomposites and nanoparticles in the plasma field [30–32]. The LPP process can easily produce nanostructures using a single process with various precursors and without adding a reducing agent.

In this study, a visible light-responsive photocatalyst was prepared by precipitating europium (Eu) on TiO<sub>2</sub>, using the LPP process. The optical and physicochemical properties of the Eu doped TiO<sub>2</sub> photocatalyst (EDTP) were measured using various analyzers.

Photodegradation activity of the synthesized EDTP was evaluated with the bare TiO<sub>2</sub> photocatalyst in UV and visible light. The photodegradation mechanism was investigated by analyzing the intermediates generated from the decomposition of ASA using the EDTP.

## **2. Materials and methods**

### **2.1 Materials**

TiO<sub>2</sub> powder, the base material of the EDTP and commercially named P-25 (anatase 85% and rutile 15% mixture, average particle size 25 nm), was obtained from and manufactured by Degussa Corporation (Germany). The Eu precursor used as a dopant was EuCl<sub>3</sub> · 6H<sub>2</sub>O and obtained from Sigma-Aldrich Corporation (USA). Deionized (DI) water, obtained from Daejung Company (Korea), having a conductivity of 2 siemens/cm or less was used to prepare an aqueous reactant solution. The photocatalytic degradation target aqueous reactant solution was prepared using ASA (C<sub>9</sub>H<sub>8</sub>O<sub>4</sub>) purchased from Sigma-Aldrich Corporation (USA).

### **2.2. Preparation of EDTP**

Europium was precipitated on TiO<sub>2</sub> powder by applying the LPP process, and a schematic of the LPP system used in this study is shown in Fig. S1 (supplementary material). A cylindrical batch reactor made of quartz was filled with an aqueous reactant solution in which TiO<sub>2</sub> powder and Eu precursor were dispersed, and plasma was generated in the solution. A tungsten electrode with a thickness of 2 mm wrapped in an insulator in the middle part of the reactor is located on both sides while maintaining an inter-electrode spacing of 1 mm, and a

high voltage is supplied using a power supply to form a plasma field. (S1 (c)). The aqueous reactant solution was maintained at 288 K using a cooling bath and was circulated to the reactor. In this study, direct pulse type electric plasma was used to prevent electrode corrosion and to clean electrode tips. The pulse width applied in the experiment was 5  $\mu$ s (S1 (b)), and the frequency and applied voltage were maintained at 30 kHz and 250 V, respectively. Photo S1 (a) showed the plasma generated between the tungsten electrode tips. Similar LPP devices have been used in previous studies, and detailed specifications and operating methods are described in the literature [28,32].

P-25 (0.5 g), the base material, was added to DI water (250 ml), followed by stirring for 300 sec, and sonification for 120 sec in to prepare a solution in which TiO<sub>2</sub> powder was uniformly dispersed. EuCl<sub>3</sub> was added to the prepared solution at a constant concentration (5 and 10 mM), and then stirred for 10 min to completely dissolve the resulting LPP aqueous reactant solution. After adding the prepared aqueous reactant solution to a quartz reactor, plasma was generated for 1 h to precipitate Eu on TiO<sub>2</sub> powder. At the end of the LPP reaction, the aqueous reactant solution was separated into a solution and a precipitate by centrifugation ( $\times$ 10,000 rpm). The separated precipitate was washed with DI water and centrifuged three times to remove unreacted impurities. The final precipitate was dehydrated using a vacuum dryer at 383 K for 24 h.

### **2.3. Determination of photocatalytic activity**

The photocatalytic activity of EDTPs prepared by the LPP method was evaluated using ASA, one of the PWWs detected in the water environment. Photocatalytic decomposition of ASA using the EDTP was carried out using UV LED and blue LED light sources. The LED light source photocatalytic decomposition apparatus is shown in Fig. S2 (c). The external photograph of the light source module equipped with 100 LED lamps used for the



photocatalysis reaction (S2 (a)) and the internal photograph of the light source module with the LED lamps turned on are shown in Fig. S2 (b). Table 1 shows the optical characteristics of the LED lamps used in the LED light module manufactured in this study.

ASA photocatalysis using the EDTP proceeded as follows. An ASA solution of 1,000 ppm concentration was prepared as a stock solution, and 0.6 L of ASA solution of 50 ppm concentration was prepared by diluting it 20 times in the decomposition reaction experiment. 0.3 g of the EDTP was added to the ASA solution and uniformly dispersed by stirring. The ASA solution in which EDTP was dispersed was put in a solution storage tank and circulated in a photoreactor using a roller pump to cause photocatalytic decomposition of ASA. The circulation flow rate of the aqueous reactant solution was 500 ml/min, and samples were taken at regular time intervals. Samples were collected by centrifugation and syringe filter to remove the EDTP in solution and then the ASA concentration was measured. High-performance liquid chromatography (HPLC) (Agilent 1260 Infinity; Agilent Technologies, USA) was used to measure the ASA concentrations over the reaction times. At this point, the photocatalytic decomposition of ASA was assumed to be a pseudo 1<sup>st</sup> order degradation reaction, and the decomposition rate was calculated. The detailed conditions of the HPLC are described in the Supplementary Materials.

### **3. Results and discussion**

#### ***3.1 Characterization of the EDTP***

The chemical composition of EDTPs prepared using the LPP process, shown in Table 2, was measured by energy dispersive X-ray spectroscopy (EDS) of a field emission scanning electron microscope (FE-SEM, JEOL-JSM-7100F). The numbers attached to the EDTP

indicate the mole concentration of the Eu in the aqueous reactant solution. For bare TiO<sub>2</sub> (P-25), the atomic percentage ratios of titanium and oxygen are 33.13 and 66.87 At. %, respectively, and they correspond to the chemical structure of pure TiO<sub>2</sub>. In the case of the EDTP, the composition of Eu increased as the composition of titanium and oxygen decreased, and it increased in proportion to the concentration of the Eu in the aqueous reactant solution [33]. Eu<sup>3+</sup> ions present in the aqueous reactant solution are reduced by electrons in the plasma field and precipitated on the surface of TiO<sub>2</sub> [34,35]. Additionally, the atomic% of oxygen in EDTPs increased, and from these results, it could be inferred that the Eu precipitated on the TiO<sub>2</sub> surface was in oxide form.

To examine the morphology and elemental distribution of EDTPs prepared using the LPP process, the analysis was performed using high-resolution field emission transmission electron microscopy (HR-FETEM, JEOL-JEM-2100F) and EDS attached to HR-TEM. The TEM image shown in Fig. 1 (a) is a real image of EDTP-10 prepared by the LPP method. The particle size of the EDTP was 15–40 nm, consistent with the average size of TiO<sub>2</sub> (P-25) used as the base material. Fig. 1 (b), (c), and (d) show the EDS mapping results for the elements Ti (green dot), O (white dot) and Eu (yellow dot). This was found to be in agreement with the shape of the EDTP nanoparticle cluster in Fig. 1 (a). Additionally, it can be seen in the image (d) that the elemental Eu is very uniformly dispersed on the TiO<sub>2</sub> surface. These results indicate that Eu ions present in aqueous solution dissociated from precursors were uniformly precipitated on the TiO<sub>2</sub> surface by the LPP process.

Meanwhile, the optical emission spectrum (OES) of radicals generated in the aqueous reactant solution was measured using an optical fiber spectrometer (Avantesie, AvaSpec-3600) installed in the LPP reactor. Fig. S3 (a) shows the OES measured in the LPP reaction using DI water. In DI water, peaks due to hydroxyl radicals (309 nm), excited hydrogen (486 nm and 656 nm), and excited oxygen (777 nm and 844 nm) were observed. Fig. S3 (b) shows

the OES of the LPP reaction solution in which the Eu precursor is dissolved, and many weak peaks are formed along with the peaks observed in DI water. The spectrum at the top of Fig. S3 (b) is an enlarged spectrum of wavelengths from 380 nm to 470 nm. Peaks by Eu ions (382 nm, 393 nm, 397 nm, 413 nm, 420 nm, 444 nm, 459 nm, 463 nm, and 466 nm) were observed [36].

In this study, Raman spectroscopy with a laser wavelength of 532 nm was used for the structural characterization of EDTPs prepared by the LPP method. The Raman spectrum of bare TiO<sub>2</sub> and the EDTPs was shown in Fig. 2. Anatase TiO<sub>2</sub> is known to have six Raman-active modes ( $A_{1g} + 2B_{1g} + 3E_g$ ). The bare TiO<sub>2</sub> used in this study showed peaks at 145 nm ( $E_g$ ), 198 nm ( $E_g$ ), 399 nm ( $B_{1g}$ ), 517 nm ( $B_{1g}$ ), and 640 nm ( $E_g$ ), indicating an anatase phase [33,37]. In the Raman spectra of the EDTPs, no new peak was observed due to impurity-related modes, and only the position of the Raman peaks shifted. Especially, the  $E_g$  mode of 145  $cm^{-1}$  shifted to higher wavelengths presumably because the crystallite size decreased [38]. Additionally, the intensity decreased with increasing Eu doping composition. This is assumed to be due to the breakdown of long-range translational crystal symmetry as defects are induced in the crystal lattice [33,38].

The chemical state of the EDTP-10 synthesized by the LPP method was confirmed by XPS and is shown in Fig. 3. Fig. 3 (a) shows the survey XPS spectrum of the EDTP-10 and strong peaks due to Ti2p and O1s were observed at binding energy (BE) of 458 eV and 530 eV, respectively. Additionally, peaks by Eu3d were observed at BE 1,120 ~ 1,170 eV, and it was confirmed that Eu was doped on the TiO<sub>2</sub> surface. The chemical composition obtained from the survey XPS spectrum in Fig. 3 (a) showed similar values to the EDS results. The high-resolution XPS spectrum for the Ti2p region was shown in Fig. 3 (b). Peaks by Ti2p<sub>3/2</sub> and Ti2p<sub>1/2</sub> were observed at 458.2 eV and 463.9 eV, and the spin-orbital splitting between the two peaks was 5.7 eV. This is due to the crystal lattice of Ti<sup>4+</sup>, and no phase transition of TiO<sub>2</sub>

was caused by Eu doping [39–41]. Fig. 3 (c) is the high-resolution XPS spectrum of the O1s region. The strong peak at BE 529.4 eV represents the Ti-O bond caused by the O<sup>2-</sup> of the TiO<sub>2</sub> lattice, and the peak at 531.4 eV is due to surface hydroxy group or adsorbed oxygen [41,42]. The small peak at BE 532.7 eV is assumed to be due to the C-O bond of the carbon tape used to fix the samples [43]. In the Eu3d region spectrum in Fig. 3 (d), the peaks at BE 1125.1 eV and 1154.2 eV are peaks caused by divalent Eu (Eu<sup>2+</sup>), and the peaks at 1134.1 eV and 1164.3 eV are due to trivalent Eu (Eu<sup>3+</sup>). From the XPS analysis result, it is determined that the Eu element precipitated to the TiO<sub>2</sub> surface by the LPP process exists in the form of europium oxide [44–47].

In this study, the objective was to produce visible photoresponsive photocatalysts. The optical properties of bare TiO<sub>2</sub> and EDTPs were measured by UV-Vis diffuse reflectance spectroscopy (UV-DRS, Shimadzu, UV-2450), and the results are shown in Fig. 4. As the Eu element precipitates on the TiO<sub>2</sub> surface through the LPP process, the absorption peak is red shifted and determined by the Eu doping content. The red shift reduces the band gap energy by facilitating the charge-transfer transition between the conduction or valence band of the rare earth Eu and TiO<sub>2</sub>. [48]. The adsorption edges of the bare TiO<sub>2</sub> were 389 nm, and the adsorption edges of Eu doped EODTP-5 and EODTP-10 were 397 nm and 408 nm, respectively. For the band gap energies of Bare TiO<sub>2</sub> and EDTPs, the adsorption edge obtained from UV-DRS was calculated by the Kubelka-Munk formula. The calculated band gap energy of bare TiO<sub>2</sub> was 3.18 eV, and the band gap energy of Eu doped EODTP-5 (3.12 eV) and EODTP-10 (3.03 eV) decreased. From the results of the DRS analysis, it was found that the EDTP prepared by the LPP method is a photocatalyst capable of responding to visible light.

### ***3.2 Photocatalytic activity of EDTP***

In this study, the photocatalytic activity of EDTPs prepared by the LPP process was evaluated in ASA—one of the pharmaceutical ingredients. As a light source for photocatalysis, a self-made LED light module using a UV and blue LED was used. Degradation of the ASA was assumed to be a pseudo 1<sup>st</sup> order degradation reaction, and the degradation rate was measured and compared with bare TiO<sub>2</sub>. Fig. 5 shows the degradation rate in ASA degradation using the bare TiO<sub>2</sub> and EDTPs as photocatalysts under UV light ( $\lambda_{\text{max}} = 375 \text{ nm}$ ). The concentration of the ASA decreased as the decomposition occurred through excitation of the photocatalyst by UV light, and the rate of ASA degradation by the EDTPs precipitated with Eu was faster than that of the bare TiO<sub>2</sub>. As Eu is precipitated on the TiO<sub>2</sub> surface, Ti<sup>4+</sup> can be converted to Ti<sup>3+</sup> by charge compensation. Ti<sup>3+</sup> acts as a trap to increase the adsorption of the reactant, as well as to reduce the recombination of photogenerated electron-holes [42]. Eventually, the decomposition rate of ASA was accelerated by Eu precipitated in TiO<sub>2</sub>. For bare TiO<sub>2</sub>, the ASA degradation rate constant  $k$  was  $9.37 \times 10^{-3} \text{ min}^{-1}$ , and for the EDTPs it was  $10.08 \times 10^{-3} \text{ min}^{-1}$  (EDTP-5) and  $10.65 \times 10^{-3} \text{ min}^{-1}$  (EDTP- 10). The degradation rate of EDTPs was improved by about 7–14% compared to that of bare TiO<sub>2</sub> and was proportional to the precipitated amount of Eu.

The results of the ASA degradation using bare TiO<sub>2</sub> and the EDTPs under blue light ( $\lambda_{\text{max}} = 465 \text{ nm}$ ) were shown in Fig. 6. It can be seen that there is barely a decomposition of ASA by bare TiO<sub>2</sub>; the decomposition reaction rate constant  $k$  was measured as  $0.140 \times 10^{-3} \text{ min}^{-1}$ . The band gap energy of bare TiO<sub>2</sub> was 3.18 eV, which is considered to be because excitation of bare TiO<sub>2</sub> is difficult to occur by blue light. On the other hand, the decomposition reaction of ASA by the EDTPs occurred, and the decomposition reaction rate was proportional to the amount of Eu precipitated on the TiO<sub>2</sub> surface. As Eu precipitated, a new energy level was formed below the conduction band of TiO<sub>2</sub>, and the band gap energy decreased, suggesting that the EDTP is excited by blue light absorption [41]. It is also

believed that the production of superoxide radicals is increased by adsorbed oxygen enhancement with inhibition of electron-hole recombination by the electron trap effect of Eu [41,49]. Degradation rate constants  $k$  of EDTP-5 and EDTP-10 were measured to be  $0.685 \times 10^{-3} \text{ min}^{-1}$  and  $1.475 \times 10^{-3} \text{ min}^{-1}$ , respectively, and were significantly improved by 5 to 10 times compared to bare  $\text{TiO}_2$ .

In order to evaluate the reusability of EDTPs prepared by the LPP method, ASA degradation reaction was performed 10 times under UV light conditions using EDTP-5 and 10, and ASA degradation rate was measured and compared for each number of times. Compared to the case where the ASA degradation experiment was first performed and 10 times, the ASA degradation reaction rate was decreased, EDTP-5 was decreased by 3.42%, and EDTP-10 was decreased by 4.53%. On the other hand, EDTPs prepared by the LPP method showed a significant decrease in reusability at the initial stage of use, but maintained reusability beyond a certain number of uses.

### ***3.3 Mechanism of decomposed ASA by EDTP***

The decomposition of ASA was carried out using EDTP-10 prepared by the LPP method, and intermediate-byproducts generated during the reaction were measured by HPLC/MS. Table 3 shows the  $m/z$ , compound name, and chemical structure of the detected intermediate-byproducts. Four intermediate-byproducts resulting from the degradation of ASA were detected.

Based on the intermediate-byproducts obtained from LC/MS, the degradation reaction pathway of ASA using the EDTP is shown in Fig. 7. The two degradation pathways are expected to be decarboxylation or deacetylation of ASA through photocatalytic degradation by the EDTP. The first degradation pathway is decomposed to phenyl acetate (2) by decarboxylation (a) of the side chain of ASA by strong oxidizing species such as hydroxyl

radicals from the EDTP [50,51]. It is converted into phenol (4) by cleavage of C-O bond of phenyl acetate and then forms hydroquinone (5) by hydroxylation. After that, it is converted into 1,4-benzoquinone and decomposed into maleic acid and fumaric acid by a ring opening reaction [50–52]. In the second pathway, hydroxyl radicals attack the C=O bonds in the ASA side chain, resulting in deacetylation (b), which in turn converts into salicylic acid (3) [51]. Salicylic acid is subsequently converted into some phenol (4) or to 2,4-dihydroxybenzoic acid by hydroxyl radical and electrophilic addition [50, 51, 53]. 2,4-dihydroxybenzoic acid is converted to maleic acid and fumaric acid by a ring opening reaction and finally mineralized to H<sub>2</sub>O and CO<sub>2</sub> [53,54].

#### 4. Conclusion

In this study, the LPP process was introduced to precipitate Eu elements on the TiO<sub>2</sub> surface, and the photocatalytic efficiency of the prepared Eu doped TiO<sub>2</sub> was evaluated for ASA, a pharmaceutical ingredient. As the precursor's concentration increased, the amount of Eu precipitated on the TiO<sub>2</sub> surface increased. Further, it was found by EDS analysis that the precipitated Eu was in oxide form. It was observed that Eu was uniformly precipitated by the LPP method on the TiO<sub>2</sub> surface, having a size of 15 to 40 nm, using HR-TEM. No new peak was observed due to impurity-related modes in the EDTPs, but the position of the Raman peak shifted to a higher wavelength. From the high-resolution XPS spectrum, it was confirmed that the elemental Eu precipitated on TiO<sub>2</sub> surface by LPP process, existed in europium oxide form. The decrease in band gap energy of the EDTP was confirmed by UV-DRS analysis; the higher is the content of Eu, the lower is the band gap energy. The photocatalytic efficiency of the EDTPs was much higher than that of bare TiO<sub>2</sub> in the visible light source; the higher the content of Eu, the better is the photocatalytic activity. HPLC/MS

was used to detect four intermediate-byproducts generated in the decomposition of ASA, and based on this, two degradation pathways were predicted. It was finally mineralized to CO<sub>2</sub> and H<sub>2</sub>O following two decomposition pathways by decarboxylation and deacetylation when attacked by hydroxyl radicals (HO·). Through this study, it was confirmed that photocatalytic efficiency can be improved and visible light response photocatalysts can be applied by doping rare earth elements on the TiO<sub>2</sub> surface, and it is considered to be applicable to fields such as decomposition of environmental pollutants.

CRedit author statement

**Sang-Chul Jung:** Conceptualization, Investigation, Data curation, Writing- Original draft preparation, Writing- Review and Editing

**Hye-Jin Bang:** Investigation, Data curation, .

**Heon Lee:** Investigation, Data curation.

**Hyung-Ho Ha:** Data curation, Validation

**Young Hyun Yu:** Data curation, Validation

**Sun-Jae Kim:** Data curation, Validation

**Young-Kwon Park:** Conceptualization, Data curation, Validation, Writing- Original draft preparation, Writing- Review and Editing

Declaration of interests

The authors declare that they have no known competing financial interests or personal relationships that could have appeared to influence the work reported in this paper.

## Acknowledgment

This research was supported by Basic Science Research Program through the National Research Foundation of Korea (NRF) funded by the Ministry of Education (NRF-2018R1D1A1B07049595).



Journal Pre-proof

## References

- [1] T. Takagi, C. Ramachandran, M. Bermejo, S. Yamashita, L. Yu, G. Amidon, *Mol. Pharm.* 3 (2006) 631-643.
- [2] B. Halling-Sorensen, S. Nors, P. Lanzky, F. Ingerslev, H. Holten, S. Jorgensen, *Chemosphere* 36 (1998) 357-393.
- [3] C.D. Daughton, T. Ternes, *Environ. Health Perspect.* 107 (1999) 907-938.
- [4] M. Carballa, F. Omil, J. Lema, M. Llompart, C. Garcí'a-Jares, I. Rodríguez, M. Go'mez, T. Ternes, *Water Res.* 38 (2004) 2918-2926.
- [5] M. Gros, M. Petrovic, A. Ginebreda, D. Barceló, *Environ. Int.* 36 (2010) 15-26.
- [6] K. Fent, A. Weston, D. Caminada, *Aquat. Toxicol.* 76 (2006) 122-159.
- [7] M. Carballa, F. Omill, J. Lema, *Water Res.* 30 (2005) 4790-4796.
- [8] D. Kanakaraju, B.D. Glass, M. Oelgemoller, *J. Environ. Manag.* 219 (2018) 189-207.
- [9] S.C. Jung, H.J. Bang, H. Lee, H. Kim, H.H. Ha, Y.H. Yu, Y.K. Park, *Sci. Total Environ.* 708 (2020) 135216.
- [10] A. Assadi, A. Eslami, *Environ. Eng. Manag. J.* 9 (2010) 807-812.
- [11] E.M. Cuerda-Correa, M.F. Alexandre-Franco, C. Fernández-González, *water* 12 (2020) 102.
- [12] H. Lee, Y.K. Park, S.J. Kim, B.H. Kim, H.S. Yoon, S.C. Jung, *J. Ind. Eng. Chem.* 35 (2016) 205-210.
- [13] S.J. Ki, Y.K. Park, J.S. Kim, W.J. Lee, H. Lee, S.C. Jung, *Chem. Eng. J.* 377 (2019)

120087.

- [14] H. Yang, G. Li, T. An, Y. Gao, J. Fu, *Catal. Today* 153 (2010) 200-207.
- [15] H. Lee, S.H. Park, Y.K. Park, S.J. Kim, S.G. Seo, S.J. Ki, S.C. Jung, *Chem. Eng. J.* 278 (2015) 259-264.
- [16] S. Jeong, H. Lee, H. Park, K.J. Jeon, Y.K. Park, S.C. Jung, *Catal. Today* 307 (2018) 65-72.
- [17] K. Hashimoto, H. Irie, A. Fujishima, *Jpn. J. Appl. Phys.* 44 (2005) 8269-8285.
- [18] M. Pelaez, N.T. Nolan, S.C. Pillai, M.K. Seery, P. Falaras, A.G. Kontos, P.S.M. Dunlop, J.W.J. Hamilton, J. Anthony Byrne, K. O'Shea, M.H. Entezari, D.D. Dionysiou, *Appl. Catal. B-Environ.* 125 (2012) 331-349.
- [19] H. Xu, S. Ouyang, L. Liu, P. Reunchan, N. Umezawa, J. Ye, *J. Mater. Chem.* 2 (2014) 12642-12661.
- [20] S. Bagheri, A. TermehYousefi, T.O. Do, *Catal. Sci. Technol.* 20 (2017) 4548-4569.
- [21] S.J. Ki, K.J. Jeon, Y.K. Park, S. Jeong, H. Lee, S.C. Jung, *Catal. Today* 293 (2017) 15-22.
- [22] H. Lee, Y.K. Park, J.S. Kim, Y.H. Park, S.C. Jung, *Environ. Res.* 169 (2019) 256-260.
- [23] J. Wang, N. Tafen, J.P. Lewis, Z. Hong, A. Manivannan, M. Zhi, M. Li, N. Wu, *J. Am. Chem. Soc.* 131 (2009) 12290-12297.
- [24] J. Matosa, A. Garcia, L. Zhao, M.M. Titirici, *Appl. Catal. A-Gen.* 390 (2010) 175-182.
- [25] H. Lee, I.S. Park, H.J. Bang, Y.K. Park, H. Kim, H.H. Ha, B.J. Kim, S.C. Jung, *Appl. Surf. Sci.* 471 (2019) 893-899.
- [26] L. Lin, Y.C. Chai, Y.C. Yang, X. Wang, D.N. He, Q.W. Tang, S. Ghoshroy, *Int. J.*

- Hydrogen Energ. 38 (2013) 2634-2640.
- [27] S. H. Sun, S. C. Jung, Korean J. Chem. Eng. 33 (2016) 1075-1079.
- [28] H. Lee, Y.K. Park, S.J. Kim, B.H. Kim, S.C. Jung, Surf. Coat. Tech. 307 (2016) 1018-1023.
- [29] W.J. Lee, S. Jeong, H. Lee, B.J Kim, K.H. An, Y.K. Park, S.C. Jung, Korean J. Chem. Eng. 34 (2017) 2993-2998.
- [30] S. Horikoshi, N. Serpone, RSC Adv. 75 (2017) 47196-47218.
- [31] Q. Chen, J. Li, Y. Li, J. Phys. D: Appl. Phys. 48 (2015) 424005.
- [32] H. Lee, S.H. Park, S.J. Kim, Y.K. Park, B.J. Kim, K.H. An, S.J. Ki, S.C. Jung, Int. J. Hydrogen Energ. 40 (2015) 754-759.
- [33] M. Pal, U. Pal, J.M.G.Y. Jiménez, F. Pérez-Rodríguez, Nanoscale Res. Lett. 7 (2012) 1.
- [34] S. Pitchaimuthu, K. Honda, S. Suzuki, A. Naito, N. Suzuki, K. Katsumata, K. Nakata, N. Ishida, N. Kitamura, Y. Idemoto, T. Kondo, M. Yuasa, O. Takai, T. Ueno, N. Saito, A. Fujishima, C. Terashima, ACS Omega 3 (2018) 898-905.
- [35] M.K. Mun, W.O. Lee, J.W. Park, D.S. Kim, G.Y. Yeom, D.W. Kim, Appl. Sci. Conver. Technol. 26 (2017) 164-173.
- [36] J.E. Sansonetti, W.C. Martin, J. Phys. Chem. Ref. Data 34 (2005) 1559-2005.
- [37] Y. Zhang, W. Wu, K. Zhang, C. Liu, A. Yu, M. Peng, J. Zhai, Phys. Chem. Chem. Phys. 18 (2016) 32178-32184.
- [38] D. Komaraiah, E. Radha, J. James, N. Kalarikkal, J. Sivakumar, M.V. Ramana Reddy, R. Sayanna, J. Lumin. 211 (2019) 320-333.

- [39] D. Xue, J. Luo, Z. Li, Y. Yin, J. Shen, *Coatings* 10 (2020) 75.
- [40] S. Anwer, G. Bharath, S. Iqbal, H. Qian, T. Masood, K. Liao, W.J. Cantwell, J. Zhang, L. Zheng, *Electrochim. Acta.* 283 (2018) 1095-1104.
- [41] M. Myilsamy, M. Mahalakshmi, N. Subha, A. Rajabhuvaneswari, V. Murugesan, *RSC Adv.* 6 (2016) 35024-35035.
- [42] D. Chen, Q. Zhu, Z. Lv, X. Deng, F. Zhou, Y. Deng, *Mater. Res. Bull.* 47 (2012) 3129-3134.
- [43] Y. Cong, X. Li, Y. Qin, Z. Dong, G. Yuan, Z. Cui, X. Lai, *Appl. Catal. B-Environ.* 107 (2011) 128-134.
- [44] J. Qi, T. Matsumoto, M. Tanaka, Y. Masumoto, *J. Phys. D Appl. Phys.* 33 (2000) 2074-2078.
- [45] W.Q. Liu, D. Wu, H. Chang, R.X. Duan, W.J. Wu, G. Amu, K.F. Chao, F.Q. Bao, O. Tegus, *nanomaterials-Basel* 8 (2018) 66.
- [46] C.H. Zeng, K. Zheng, K.L. Lou, X.T. Meng, Z.Q. Yan, Z.N. Ye, R.R. Su, S. Zhong, *Electrochim. Acta* 165 (2015) 396-401.
- [47] I. Camps, M. Borlaf, M. T. Colomer, R. Moreno, L. Duta, C. Nita, A. Perez del Pino, C. Logofatu, R. Serna, E. Gyorgy, *RSC Adv.* 7 (2017) 37643-37653.
- [48] G.V. Khade, N.L. Gavade, M.B. Suwarnkar, M.J. Dhanavade, K.D. Sonawane, K.M. Garadkar, *J. Mater. Sci-Mater. El.* 28 (2017) 11002-11011.
- [49] P. Yang, C. Lu, N. Hua, D. Yukou, *Mater. Lett.* 57 (2002) 794-801.
- [50] L. Li, Q. Ma, S. Wang, S. Song, B. Li, R. Guo, X. Cheng, Q. Cheng, *catalysts* 8 (2018)

118.

[51] Y. Cui, Q. Meng, X. Deng, Q. Ma, H. Zhang, X. Cheng, X. Li, M. Xie, Q. Cheng, *J. Ind. Eng. Chem.* 43 (2016) 177-184.

[52] D. Mukherjee, A.K. Ray, S. Barghi, *processes*, 4 (2016) 13.

[53] Q. Dai, Y. Xia, L. Jiang, W. Li, J. Wang, J. Chen, *Int. J. Electrochem. Sci.* 7 (2012) 12895-12906.

[54] W. Wang, Q. Zhu, F. Qin, Q. Dai, X. Wang, *Chem. Eng. J.* 333 (2018) 226-239.

Journal Pre-proof

### Captions for Figures

Fig. 1. HR-TEM real image (a), Ti element mapping (b), O element mapping (c) and Eu element mapping (d) of EDTP-10 prepared using LPP process.

Fig. 2. Raman spectra of Eu-doped TiO<sub>2</sub> photocatalysts and bare TiO<sub>2</sub>.

Fig. 3. XPS spectrum of EDTP-10 prepared using the LPP process: survey (a), Ti2p (b), O1s (c), and Eu3d (d).

Fig. 4. Comparison of diffuse reflectance spectrum of bare TiO<sub>2</sub> and prepared EDTPs.

Fig. 5. ASA degradation rate of bare TiO<sub>2</sub> and EDTPs using UV LED light source.

Fig. 6. ASA degradation rate of bare TiO<sub>2</sub> and EDTPs under blue LED light conditions.

Fig. 7. Proposed pathways for the photocatalytic degradation of ASA.

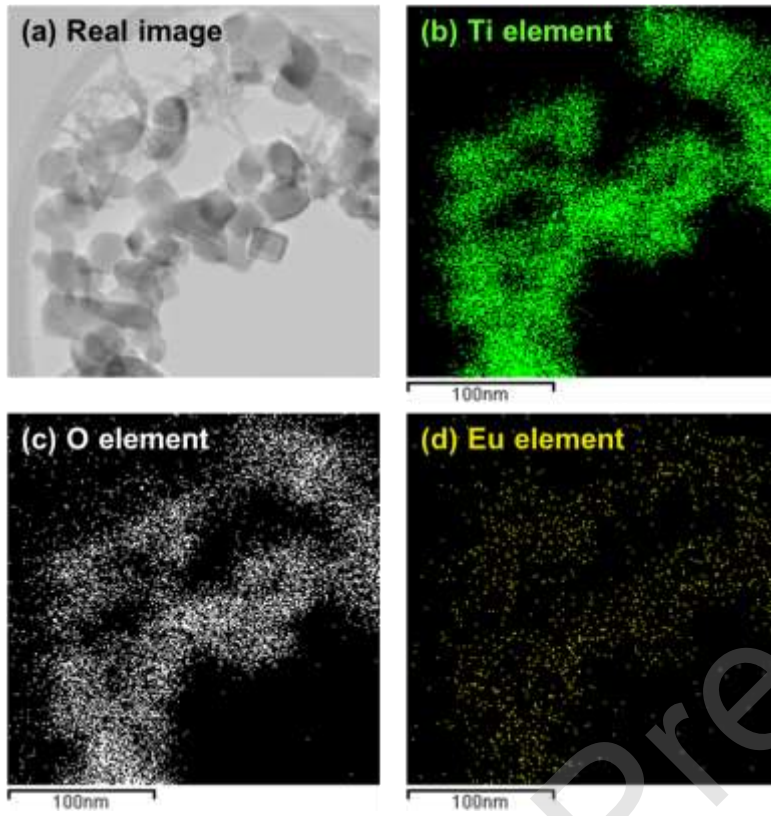


Fig. 1. Jung et al.,



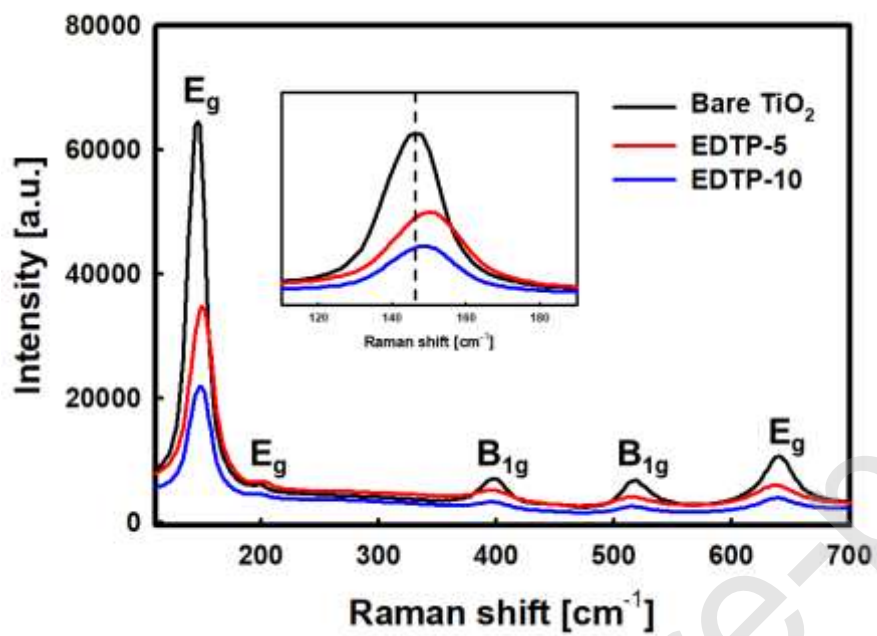


Fig. 2. Jung et al.,

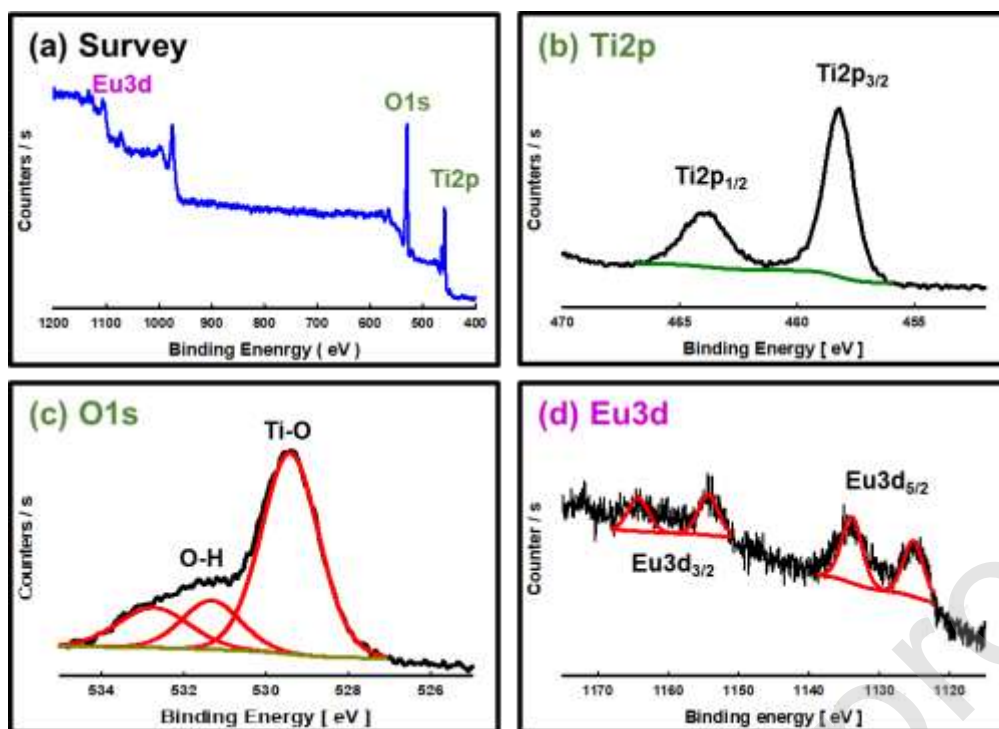


Fig. 3. Jung et al.,

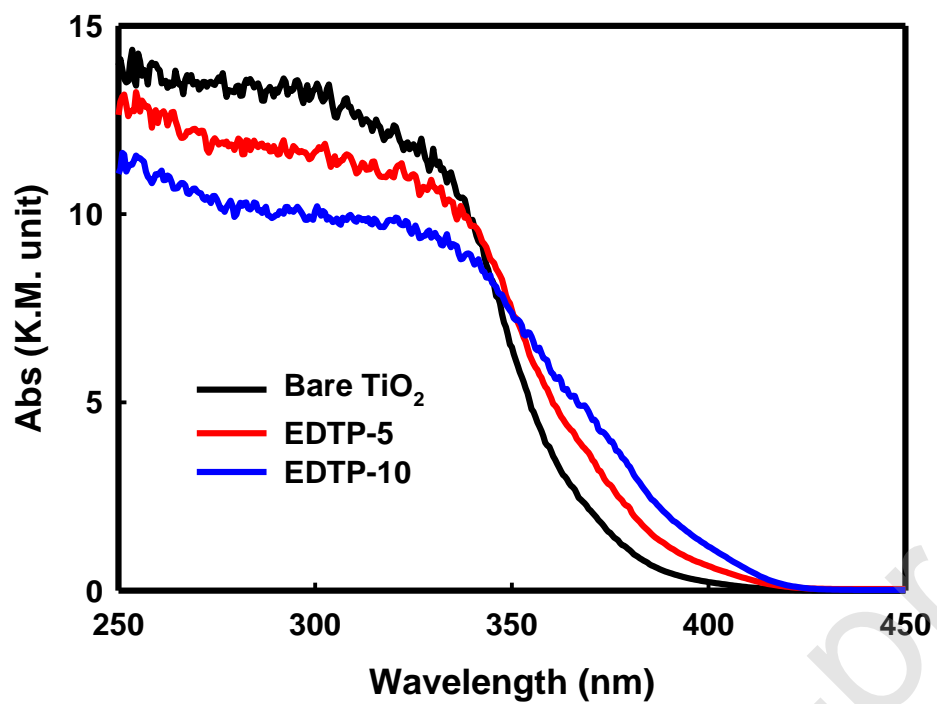


Fig. 4. Jung et al.,

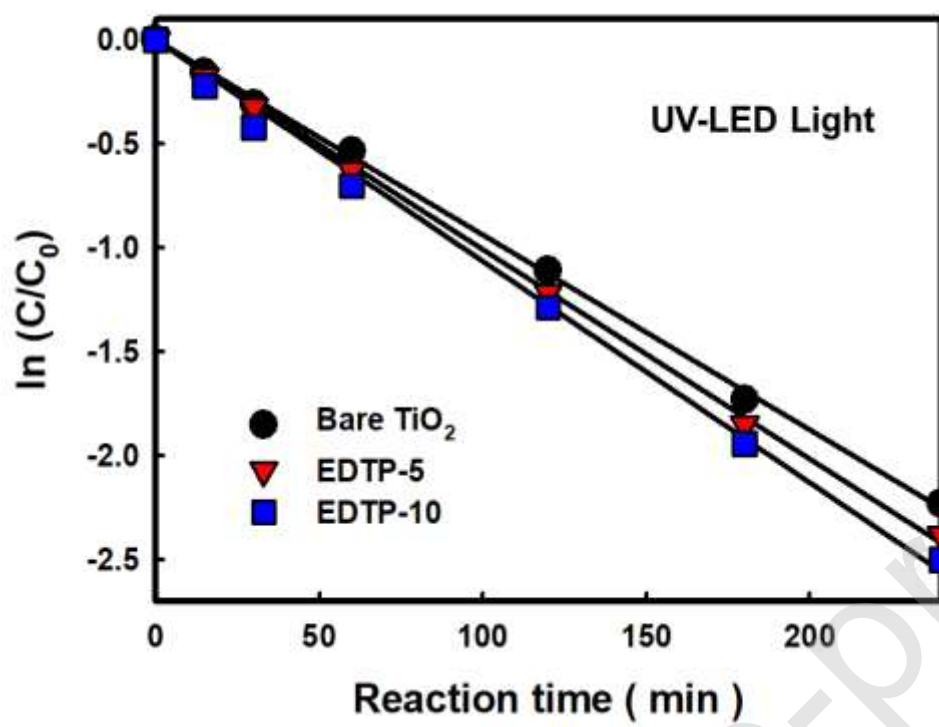


Fig. 5. Jung et al.,

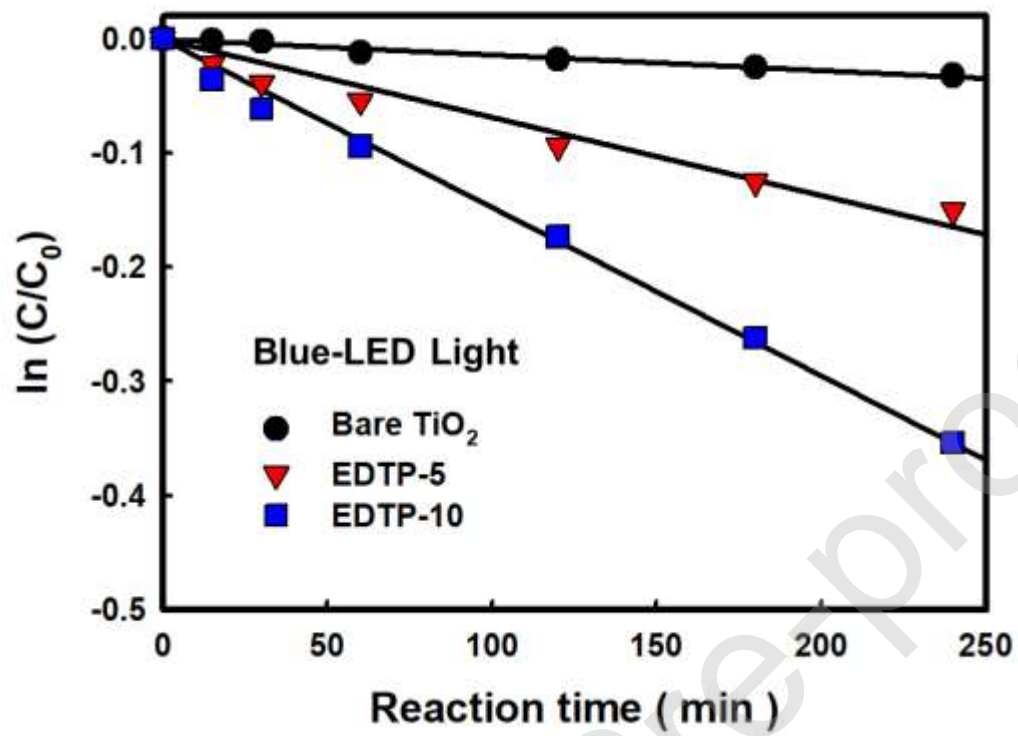


Fig. 6. Jung et al.,

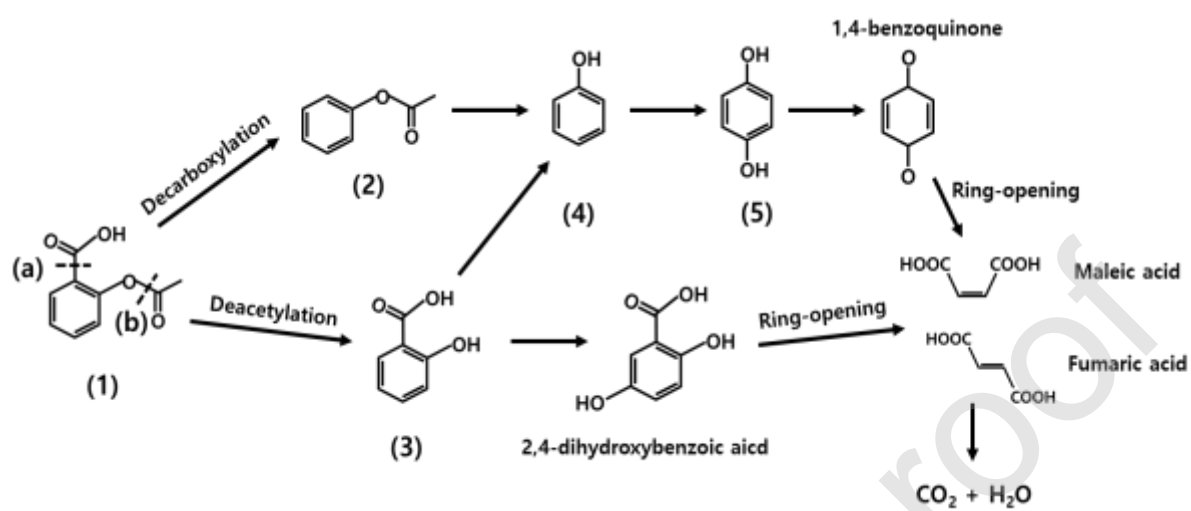


Fig. 7. Jung et al.,

Table 1. Specification of UV and blue LED used in this work.

Light type	$P_D$ (Power dissipation)	$\Phi_e$ (Radiant Flux)	$I_v$ (Luminous intensity)	$\lambda$ (Wavelength)	$\lambda_p$ (Peak wavelength)
UV-LED ( NSPU510CS, Nichia)	80 mW	7,500 $\mu$ W		360 ~ 390 nm	375 nm
Blue-LED ( NSPB510BS, Nichia)	120 mW		4.7 cd	440 ~ 500 nm	465 nm

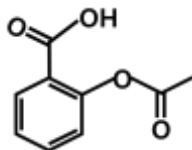
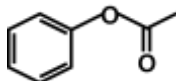
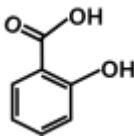
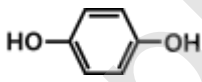
The LED light module was arranged in  $10 \times 10$  lines using 100 UV LEDs and blue LEDs, respectively. The power dissipation of the UV and blue LED light modules was 8,000 mW and 12,000 mW, respectively.

Table 2. Chemical composition of bare TiO<sub>2</sub> with EDTPs prepared by LPP process.

Sample	Initial precursor Concentration (mM)	Titanium		Oxygen		Europium	
		Wt. %	At. %	Wt. %	At. %	Wt. %	At. %
Bare TiO <sub>2</sub>	0	59.73	33.13	40.27	66.87	0.00	0.00
EDTP-5	5	58.64	32.81	39.97	66.95	1.39	0.24
EDTP-10	10	57.30	32.34	39.73	67.13	2.97	0.53



Table 3. Intermediate-byproducts produced by photocatalysis of ASA with EDTP-10.

No.	$m/z$	Compound name	Chemical structure
1	179	acetylsalicylic acid (ASA)	
2	135	Phenyl acetate	
3	137	Salicylic acid	
4	93	Hydroquinone	
5	109	Phenol	